Matrix Formulation of Algebraically-Stabilized Explicit Integration for Thermonuclear Networks

Mike Guidry
Department of Physics and Astronomy, University of Tennessee
Knoxville, TN 37996-1200, USA

These notes outline a matrix reformulation of algebraically-stabilized explicit integration methods for thermonuclear networks that parallels the implementation of such methods for neutrino transport by Eirik Endeve.

1 Introduction

Problems from many scientific and technical disciplines require solving large coupled reaction networks. The differential equations used to model these networks usually exhibit *stiffness,* which arises because of multiple timescales in the problem that differ by many orders of magnitude [1, 2, 3, 4]. Astrophysical thermonuclear networks are extremely stiff, often with 10-20 orders of magnitude difference between the fastest and slowest timescales. Standard explicit numerical integration schemes such as the forward Euler method cannot deal efficiently with stiff systems because stability requires timesteps that are far too small to be practical. For more than half a century stiff systems have been integrated using some variant of implicit methods. These are stable for reasonable timesteps but increasingly inefficient for large networks because they require (typically several) matrix inversions at each integration step, causing compute time to scale from quadratically to cubically with the number of species in the network unless sparse-matrix methods can be applied [5, 6].

More recently it has been shown that modified explicit methods employing algebraic constraints to stabilize against the stiffness instability permit explicit timesteps comparable to those for implicit methods, with much faster computation of each timestep for large networks because no matrix inversions are required [7, 8, 9, 10, 11, 12]. For an N-species network the equations to be solved have the generic form

$$\begin{aligned}\frac{dy_i}{dt} &= F_i^+ - F_i^- = (f_1^+ + f_2^+ + \ldots)_i - (f_1^- + f_2^- + \ldots)_i \\ &= (f_1^+ - f_1^-)_i + (f_2^+ - f_2^-)_i + \ldots = \sum_j (f_j^+ - f_j^-)_i,\end{aligned} \tag{1}$$

where the $y_i (i = 1 \ldots N)$ describe the species abundances, t is the time, the total flux depleting species i is F_i^- and the total flux increasing it is F_i^+, the fluxes between species i and j are denoted by $(f_j^\pm)_i$, and the sum for each variable i is over all variables j coupled to i by a non-zero flux $(f_j^\pm)_i$. In Eq. (1) two ways to group the terms on the right side have been indicated, with the first line representing a decomposition into total flux in and out of species i and the second line separating the total flux into in and out contributions from individual reactions. The new explicit approaches are based on the observation that for a single timestep dt in Eq. (1) the

solution for y_i has two different analytical solutions for $F_i^+ \sim F_i^-$ and another analytical solution for $f_j^+ \sim f_j^-$, and that when these conditions are fulfilled numerical integration can be replaced partially by analytical integration, thereby reducing the stiffness by removing fast timescales from the overall numerical integration. With these methods and efficient GPU acceleration, it was shown that hundreds of 150-isotope thermonuclear networks could be integrated under Type Ia supernova conditions in the same computing time required to integrate one such network with a standard implicit method [11, 12]. This orders of magnitude increase in efficiency results from a combination of (1) intrinsic speed advantages of the new explicit algorithms, by virtue of avoiding inversions of large matrices, and (2) optimal exploitation of massive parallelism for the new algorithms by saturating available GPU threads.

Recently the new explicit methods developed in Refs. [7, 8, 9, 10, 11, 12] have been reformulated in more traditional matrix language by Endeve and collaborators, and applied to the problem of neutrino transport under conditions expected for core-collapse supernovae or neutron star mergers [13]. The original formulation and this newer matrix formulation should be equivalent mathematically but the Endeve matrix formulation offers certain practical advantages:

1. It is closer formally to the implementation of the problem in standard codes, allowing easier comparison of the newer methods with traditional methods. This can facilitate the porting of the new explicit approach to a variety of problems in various fields.

2. It can leverage optimized standard linear algebra packages in implementing algebraically-stabilized explicit integration (but requires only matrix-vector multiplies and no matrix inversions).

3. It is an instructive way to visualize some aspects of the problem, such as the approach to microscopic and macroscopic equilibrium.

4. It makes clear a connection between these new explicit approaches and fixed point methods that may be of some use computationally.

For these reasons, it is useful to reformulate the algorithm for thermonuclear networks demonstrated in Refs. [7, 8, 9, 10, 11, 12] using the matrix algorithm of [13]. These notes outline that reformulation.

2 Differential Equations and Rates

As in the original formulation of the explicit algebraic thermonuclear network in Ref. [7], we shall use the ReacLib nuclear reaction library [14] to supply rates for astrophysical thermonuclear reactions.

2.1 Reaction Rates Using the ReacLib Library

In the ReacLib rate library nuclear reactions of importance in astrophysics are assigned to *eight reaction classes,* depending on the number of *nuclear species* on the two sides of the reaction

Table 1: ReacLib reaction classes [14]

Class	Reaction	Description or example
1	a $\rightarrow$ b	β-decay or e$^-$ capture
2	a $\rightarrow$ b + c	Photodisintegration + α
3	a $\rightarrow$ b + c + d	^{12}C $\rightarrow 3\alpha$
4	a + b $\rightarrow$ c	Capture reactions
5	a + b $\rightarrow$ c + d	Exchange reactions
6	a + b $\rightarrow$ c + d + e	^{2}H + ^{7}Be $\rightarrow$ ^{1}H + 2^{4}He
7	a + b $\rightarrow$ c + d + e + f	^{3}He + ^{7}Be $\rightarrow$ 2^{1}H + 2^{4}He
8	a + b + c $\rightarrow$ d (+ e)	Effective 3-body reactions

equation,[1] as illustrated in Table 1.

1. ReacLib reaction classes 1-3 are termed *one-body* because there is one nuclear species on the left side of the reaction equation.

2. ReacLib classes 4-7 are termed *two-body* because there are two nuclear species on the left side.

3. ReacLib class 8 is termed *three-body* because there are three nuclear species on the left side.

The total rate R^α for a nuclear reaction in ReacLib labeled by an index or label α uniquely identifying the reaction and is expressed in terms of a sum over components R_k^α

$$R^\alpha = \sum_k R_k^\alpha, \tag{2}$$

where each component R_k^α has a temperature dependence that is parameterized in the form

$$R_k^\alpha = \exp\left(P_{1k}^\alpha + \frac{P_{2k}^\alpha}{T_9} + \frac{P_{3k}^\alpha}{T_9^{1/3}} + P_{4k}^\alpha T_9^{1/3} + P_{5k}^\alpha T_9 + P_{6k}^\alpha T_9^{5/3} + P_{7k}^\alpha \ln T_9\right), \tag{3}$$

where T_9 is the temperature in units of 10^9 K and the seven parameters $P_{nk}^\alpha (n = 1,2,\ldots 7)$ for a given reaction α and component k are constants tabulated in the ReacLib library for each reaction. In some cases a single component R_k^α is sufficient to parameterize a rate but often several terms R_k^α are required to cover a temperature range. ReacLib parameters for an example reaction parameterized by two components are shown in Table 2, and the corresponding reaction rate computed from Eqs. (2) and (3) is shown as a function of temperature in Fig. 1.[2] In this example the index α labels the reaction ^{12}C$(\alpha,\gamma)^{16}$O and the index $k = 1,2$ labels the two components of the reaction tabulated in ReacLib and displayed in Table 2.

[1] Thus photons (γ), neutrinos (ν or $\bar{\nu}$), electrons (e^- or β^-), and positrons (e^+ or $\beta+$) don't count in this classification.

[2] Notice that in Fig. 1 a change of one order of magnitude in T changes the reaction rate by seven orders of magnitude. This illustrates the necessity of a parameterization that can accommodate very large changes of rates with temperature, and is one reason why several components R_k^α may be necessary in the sum of Eq. (2) to parameterize rates over the range of temperatures $T = 10^7 - 10^{10}$ K for which ReacLib is expected to be valid.

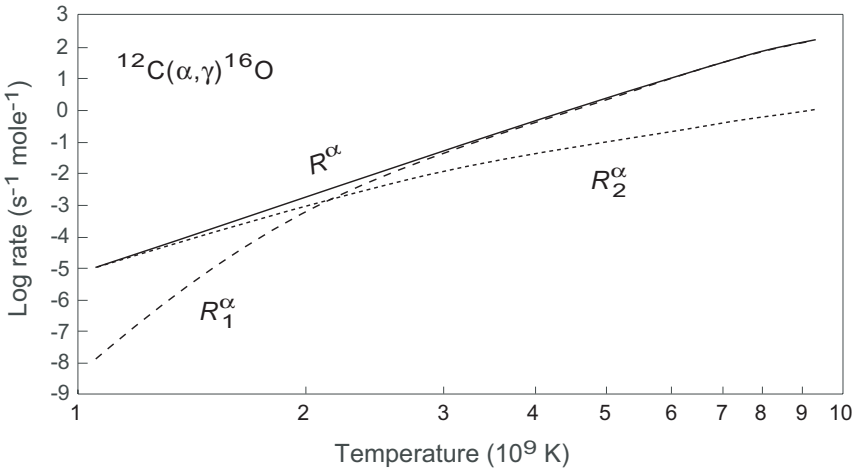

Figure 1: Total reaction rate R^{α} for $^{12}\mathrm{C}(\alpha,\gamma)^{16}\mathrm{O}$ expressed in terms of two components R^{α}_{k} in the ReacLib parameterization of Eqs. (2)–(3) that are given in Table 2.

Table 2: ReacLib P^{α}_{nk} for $^{12}\mathrm{C}(\alpha,\gamma)^{16}\mathrm{O}$ labeled by reaction index α and component index k

k	P^{α}_{1k}	P^{α}_{2k}	P^{α}_{3k}	P^{α}_{4k}	P^{α}_{5k}	P^{α}_{6k}	P^{α}_{7k}
1	18.4977	0.0048	−33.2522	3.3352	−0.7017	0.0782	−2.8075
2	142.191	−89.1608	2204.35	−2380.31	108.931	−5.3147	1361.18

2.2 Network Differential Equations

With the rates parameterized in terms of the ReacLib library it is convenient to write the coupled set of N differential equations describing the thermonuclear network for N isotopic species in the form [5]

$$\dot{Y}_i = \sum_j \eta^i_j \lambda_j Y_j + \sum_{jk} \eta^i_{jk} \rho N_{\mathrm{A}} \langle jk \rangle Y_j Y_k + \sum_{jk\ell} \eta^i_{jk\ell} \rho^2 N^2_{\mathrm{A}} \langle jk\ell \rangle Y_j Y_k Y_\ell \qquad (i = 1,2,\ldots N), \quad (4)$$

where the three terms represent one-body, two-body, and three-body reactions, respectively, that alter the abundance of species i, the sums represent contributions from all reactions that can increase or decrease Y_i, $\dot{Y}_i \equiv dY_i/dt$, and where

1. Avogadro's constant is $N_{\mathrm{A}} = 1/M_\mu = 6.0221409 \times 10^{23}$ mol^{-1}, where $M_\mu = 1.6605390 \times 10^{-24}$ g is the atomic mass unit (amu).

2. The abundance Y_i of species i is defined by

$$Y_i \equiv \frac{X_i}{A_i} = \frac{n_i}{\rho N_{\mathrm{A}}}, \quad (5)$$

where X_i is the mass fraction, A_i is the atomic mass number, n_i is the number density for species i, and ρ is the mass density.

3. The η factors are constants that account for the signs of the terms and for counting particles (while avoiding double counting of identical particles) that are given by

$$\eta_j^i = \text{sgn} \times N_i \qquad \eta_{jk}^i = \text{sgn} \times \frac{N_i}{M!} \qquad \eta_{jk\ell}^i = \text{sgn} \times \frac{N_i}{M!}, \tag{6}$$

where N_i is the number of particles of species i created or destroyed in a single reaction, M is the number of identical particles in the entrance channel, and sgn is $+1$ if the reaction increases Y_i (a source) and -1 if it decreases Y_i (a sink).

4. The parameter λ_j is a one-body decay rate, $\langle jk \rangle$ is the velocity-averaged two-body reaction rate, and $\langle jk\ell \rangle$ is a corresponding velocity-averaged three-body reaction rate.

The parameterized rates R^α of Eqs. (2)-(3) that are computed using the ReacLib library are defined such that they have the following correspondence with rates λ_i, $\langle jk \rangle$, and $\langle jk\ell \rangle$ appearing in Eq. (4):

$$R_{(1)}^\alpha = \lambda_i \qquad \left(\text{1-body, with units } \text{s}^{-1} \right) \tag{7a}$$

$$R_{(2)}^\alpha = N_\text{A} \langle jk \rangle \qquad \left(\text{2-body, with units } \text{cm}^3\text{mol}^{-1}\text{s}^{-1} \right) \tag{7b}$$

$$R_{(3)}^\alpha = N_\text{A}^2 \langle jk\ell \rangle \qquad \left(\text{3-body, with units } \text{cm}^6\text{mol}^{-2}\text{s}^{-1} \right) \tag{7c}$$

where $R_{(n)}^\alpha$ refers to Eq. (2) evaluated for the n-body reaction labeled by index α.[3] Then Eq. (4) may be rewritten

$$\dot{Y}_i = \sum_j \left(\eta_j^i R_{(1)}^\alpha \right) Y_j + \sum_j \left(\sum_k \eta_{jk}^i \rho R_{(2)}^\alpha Y_k \right) Y_j + \sum_j \left(\sum_{k\ell} \eta_{jk\ell}^i \rho^2 R_{(3)}^\alpha Y_k Y_\ell \right) Y_j, \tag{8}$$

in terms of rates $R_{(n)}^\alpha$ that may be computed from the ReacLib library for given temperature and density conditions. In general the quantities in parentheses in Eq. (8) have the units of inverse seconds, so that quantities on the right side match the units of $\dot{Y}_i = dY_i/dt$ on the left side.

2.3 Matrix Formulation of the Network

We may write Eq. (8) as $\dot{Y}_i = \sum_j M_{ij} Y_j$, or explicitly as the matrix equation

$$\begin{pmatrix} \dot{Y}_1 \\ \dot{Y}_2 \\ \dot{Y}_3 \\ \vdots \\ \dot{Y}_N \end{pmatrix} = \begin{pmatrix} M_{11} & M_{12} & M_{13} & \cdots & M_{1N} \\ M_{21} & M_{22} & M_{23} & \cdots & M_{2N} \\ M_{31} & M_{32} & M_{33} & \cdots & M_{3N} \\ \vdots & \vdots & \vdots & \cdots & \vdots \\ M_{N1} & M_{N2} & M_{N3} & \cdots & M_{NN} \end{pmatrix} \begin{pmatrix} Y_1 \\ Y_2 \\ Y_3 \\ \vdots \\ Y_N \end{pmatrix}, \tag{9}$$

[3] The subindex (n) should not be confused with the subindex k in Eq. (3). It is somewhat redundant since the label α specifies the reaction, but it is useful in the present discussion to display whether the reaction is 1-body, 2-body, or 3-body because these correspond to different terms in Eq. (4), and different definitions in Eq. (7).

where the elements of the matrix M_{ij} are defined by a sum of 1-body, 2-body, and 3-body terms,

$$M_{ij} = M_{ij}^{(1)} + M_{ij}^{(2)} + M_{ij}^{(3)}, \tag{10}$$

which we can express as

$$M_{ij}^{(1)} = \eta_j^i R_{(1)}^\alpha \qquad M_{ij}^{(2)} = \sum_k \eta_{jk}^i \rho R_{(2)}^\alpha Y_k \qquad M_{ij}^{(3)} = \sum_{k\ell} \eta_{jk\ell}^i \rho^2 R_{(3)}^\alpha Y_k Y_\ell, \tag{11}$$

in terms of the rates $R_{(n)}^\alpha$ evaluated from ReacLib in Eqs. (2) and (3) for 1-body, 2-body, and 3-body terms, the mass density ρ, the isotopic abundances Y_i, and the bookkeeping η-factors, which are constants for each reaction in a given network.[4] The fluxes M_{ij} in Eqs. (10) and (11) have units of s^{-1}.

3 Algebraic Stabilization of Explicit Solutions

We have now formulated the thermonuclear network problem in matrix form as Eqs. (9)-(11). Let's now solve the problem within this framework using the new explicit algebraic methods developed in Refs. [7, 8, 9, 10, 11, 12]. We will give a very schematic outline of the explicit algebraic approximations to be used, with details to be found in the references. There are two fundamental sources of stiffness in Eq. (1).

1. In line one of Eq. (1) the difference of two very large numbers $F_i^+ - F_i^-$ for an isotopic species i may approach zero; we term this *macroscopic equilibration* for a species.

2. In line two of Eq. (1) the difference of two very large numbers $(f_j^+ - f_j^-)_i$ for a forward–backward reaction pair may approach zero; we term this *microscopic equilibration.*

These sources of stiffness may be ameliorated, thereby stabilizing explicit integration for large timesteps, by a combination of three approximate algebraic solutions that we now describe.

3.1 Stabilizing the Approach to Macroscopic Equilibration

The differential equations to be solved take the form given by Eq. (1). Generally, for a species i the total flux augmenting it F_i^+ and the total flux depleting it F_i^- each consist of a number of terms depending on the other populations in the network. For the networks that we shall consider the depletion flux for the population y_i will be proportional to y_i,

$$F_i^- = (k_1^i + k_2^i + \ldots + k_m^i) y_i \equiv k^i y_i, \tag{12}$$

[4]Notice the non-linearity of Eq. (9) resulting from the equation for a given $\dot{Y}_i$ having contributions depending as much as cubically on Y for it and other species in the network. In principle the sums over j,k,ℓ in Eq. (11) range over all species in the network. In practice, since most nuclear reactions important in astrophysics (fission reactions are an exception but they occur only in limited circumstances) change neutron and proton numbers by at most several, the sums are restricted but still can involve many terms. The restriction of the summations implies that the matrix M of Eq. (9) is relatively *sparse* for a large thermonuclear network, with a low density of nonzero M_{ij}.

where the k_j^i are rate parameters (in units of time^{-1}) for each of the m processes that can deplete y_i, which may depend on the populations y_j and on thermodynamical variables such as temperature and density, which affect the rates. The characteristic timescales $\tau_j^i = 1/k_j^i$ will vary over many orders of magnitude in the systems of interest, so these equations are very stiff. From Eq. (12) the effective total depletion rate k^i for y_i at a given time, and a corresponding timescale τ^i, may be defined as

$$k^i \equiv \frac{F_i^-}{y_i} \qquad \tau^i = \frac{1}{k^i}, \tag{13}$$

permitting Eq. (1) to be written as

$$y_i = \frac{1}{k^i}\left(F_i^+ - \frac{dy_i}{dt}\right). \tag{14}$$

Now consider the situation where $F_i^+ \simeq F_i^-$ for a species i, so that $dy_i/dt \to 0$.

3.1.1 Asymptotic Approximation

An approximate solution of Eq. (14) for $F_i^+ \simeq F_i^-$ in finite-difference approximation is [8]

$$y_n = \frac{1}{1+k_n\Delta t}\left(y_{n-1} + F_n^+\Delta t\right), \tag{15}$$

where n labels the current integration timestep and $n-1$ labels the preceding step. This *asymptotic approximation* is expected to be valid for $k\Delta t >> 1$. It defines an *explicit method,* since all information required to calculate y_n is known from the preceding $n-1$ step. To implement an asymptotic algorithm we define a critical value κ of $k\Delta t$ and at each timestep cycle through all populations and compute the product $k^i\Delta t$ for each species i using Eq. (13) and the proposed timestep Δt. Then, for each species i

1. If $k^i\Delta t < \kappa$, the population is updated numerically for that timestep by the explicit Euler method.

2. If $k\Delta t \geq \kappa$, the population is updated algebraically for that timestep using Eq. (15).[5]

Formally explicit numerical integration (for example, the forward Euler method) is expected to be stable if $k^i\Delta t < 1$ and unstable if $k^i\Delta t \geq 1$ (see the discussions in Refs. [1] and [8]).

3.1.2 Quasi-Steady-State Approximation

An alternative explicit algebraic solution to the coupled differential equations is possible using the quasi-steady-state (QSS) approximation [15, 16]. First notice that Eq. (1), expressed in the form

$$\frac{dy}{dt} = F^+(t) - k(t)y(t) \tag{16}$$

[5]This is the original asymptotic prescription [7]. The neutrino code is using a slight variant, so this should be updated to reflect the actual prescription in the neutrino matrix code.

using Eq. (12) and with indices dropped for notational convenience, has the general solution

$$y(t) = y_0 e^{-kt} + \frac{F^+}{k}\left(1 - e^{-kt}\right), \tag{17}$$

provided that k and F^+ are constant. (They aren't generally constant, but may be approximately constant over a single integration timestep.) This equation may then be used in a predictor–corrector algorithm in which a prediction is made using only initial values and then a corrector is applied that uses a combination of initial values and values computed using the predictor solution. Defining a parameter $\alpha(r)$ by

$$\alpha(r) = \frac{160r^3 + 60r^2 + 11r + 1}{360r^3 + 60r^2 + 12r + 1}, \tag{18}$$

where $r \equiv 1/k\Delta t$, a predictor y^{p} and a corrector y^{c} may be implemented by [15, 16]

$$y^{\mathrm{p}} = y^0 + \frac{\Delta t(F_0^+ - F_0^-)}{1 + \alpha^0 k^0 \Delta t} \qquad y^{\mathrm{c}} = y^0 + \frac{\tilde{F}^+ - \bar{k}y^0}{1 + \bar{\alpha}\bar{k}\Delta t}, \tag{19}$$

where α^0 is evaluated from Eq. (18) with $r = 1/k^0\Delta t$, an average rate parameter is defined by $\bar{k} = \frac{1}{2}(k^0 + k^{\mathrm{p}})$, $\bar{\alpha}$ is specified by Eq. (18) with $r = 1/\bar{k}\Delta t$, and

$$\tilde{F}^+ = \bar{\alpha}F_{\mathrm{p}}^+ + (1 - \bar{\alpha})F_0^+.$$

The corrector can be iterated if desired by using y^{c} from one iteration step as the y^{p} for the next iteration step, though experience so far with thermonuclear networks and with initial application of these methods to neutrino transport suggests that such iteration does not affect the results very much.

The explicit QSS algorithm is implemented essentially in the same way as the asymptotic method described above over each timestep, except that all equations are treated uniformly in QSS approximation, rather than dividing the equations into a set treated numerically by explicit forward difference and a set treated analytically [9]. Thus at each timestep all N isotopic species abundances of the network are updated analytically using the QSS approximation. Everything required for this update at timestep n is known from the preceding $n-1$ timestep, so the QSS approximation is an explicit method.

3.2 Stabilizing the Approach to Microscopic Equilibrium

Either the asymptotic or the QSS method described above work well for macroscopic equilibration, but are highly inefficient for systems experiencing microscopic equilibration. In this section approximations to stabilize explicit integration in the presence of microscopic equilibration are summarized [10].

3.2.1 Partial Equilibrium

Partial equilibrium (PE) methods examine source terms f_i^+ and f_i^- for approach to equilibrium of the *individual forward–backward reaction pairs* exhibited in the second line of Eq. (1). When a fast reaction pair is deemed to be in equilibrium its source terms are removed from the numerical integration and replaced by equilibrium algebraic constraints. This removal of fast timescales associated with equilibrating reaction pairs from the numerical integration reduces the stiffness of the equations being integrated, permitting larger stable timesteps. Let's illustrate with a 2-body reaction pair $a+b \rightleftharpoons c+d$ and its source term

$$f_{ab\rightleftharpoons cd} = \pm(k_{\rm f} y_a y_b - k_{\rm r} y_c y_d), \tag{20}$$

where y_i is a population variable for species i and the rate parameters for the forward and reverse reactions are $k_{\rm f}$ and $k_{\rm r}$, respectively. Considered in isolation for a single numerical integration step, the reaction pair of Eq. (20) may be deemed equilibrated if $f_{ab\rightleftharpoons cd} \sim 0$. Let's define *partial equilibrium (PE)* to be a situation where some reaction pairs have $f \sim 0$ and some have $f \neq 0$, with the approach to complete equilibrium then viewed as a stepwise equilibration of all forward–backward reaction pairs in the network.

3.2.2 Approach to Equilibrium for a Reaction Pair

The stoichiometry of the representative reaction $a+b \rightleftharpoons c+d$ implies the constraints

$$y_a - y_b = c_1 \qquad y_a + y_c = c_2 \qquad y_a + y_d = c_3, \tag{21}$$

where the constants c_i may be evaluated by substituting the initial abundances into Eq. (21). Defining the new constants

$$a \equiv k_{\rm r} - k_{\rm f} \qquad b \equiv -k_{\rm r}(c_2+c_3) + k_{\rm f} c_1 \qquad c \equiv k_{\rm r} c_2 c_3,$$

the evolution of y_a over the timestep is described by the differential equation

$$\frac{dy_a}{dt} = -k_{\rm f} y_a y_b + k_{\rm r} y_c y_d = a y_a^2 + b y_a + c, \tag{22}$$

with the corresponding evolution of y_b, y_c, and y_d following from the constraints (21). This result was derived specifically for the 2-body reaction $a+b \rightleftharpoons c+d$ but the approach to equilibrium for any 2-body reaction pair can be described by, and the approach to equilibrium for any 3-body reaction pair can be approximated by, a differential equation of the form (22). In terms of the quantity

$$q \equiv 4ac - b^2, \tag{23}$$

the relevant solutions of Eq. (22) correspond to $a \neq 0$ and $q < 0$, and take the form [16, 17]

$$y_a(t) = -\frac{1}{2a}\left(b + \sqrt{-q}\,\frac{1+\phi\exp(-\sqrt{-q}\,t)}{1-\phi\exp(-\sqrt{-q}\,t)}\right) \qquad \phi \equiv \frac{2ay_0 + b + \sqrt{-q}}{2ay_0 + b - \sqrt{-q}}. \tag{24}$$

The *equilibrium solution* $\bar{y}_a$ then corresponds to the limit $t \to \infty$ of Eq. (24),

$$\bar{y}_a = -\frac{1}{2a}\left(b + \sqrt{-q}\right). \tag{25}$$

Once $\bar{y}_a$ has been determined the constraints (21) may be used to determine the other equilibrium abundances:

$$\bar{y}_b(t) = \bar{y}_a(t) - c_1 \qquad \bar{y}_c(t) = c_2 - \bar{y}_a(t) \qquad \bar{y}_d(t) = c_3 - \bar{y}_a(t).$$

It is often convenient to introduce a variable λ that is the difference between the values of the y_i at the beginning of the timestep and their current values

$$y_a = y_a^0 - \lambda \qquad y_b = y_b^0 - \lambda \qquad y_c = y_c^0 + \lambda \qquad y_d = y_d^0 + \lambda. \tag{26}$$

The new variable λ is termed a *progress variable* for the reaction characterized by $f_{ab \rightleftharpoons cd}$.

Thus the approach of $a + b \rightleftharpoons c + d$ to equilibrium is controlled by a single differential equation (22) that can be expressed in terms of either a single one of the abundances y_i, or the progress variable λ. The general solution of this equation is of the form given by Eq. (24), with the time dependence residing dominantly in the exponentials. Therefore, the rate at which $a + b \rightleftharpoons c + d$ evolves toward the equilibrium solution (25) is governed by a *single timescale*

$$\tau = \frac{1}{\sqrt{-q}}, \tag{27}$$

which is illustrated in Fig. 2. Whether a reaction pair is near equilibrium at time t may then be determined by requiring that

$$\frac{|y_i(t) - \bar{y}_i|}{\bar{y}_i} < \varepsilon \tag{28}$$

for *all species i* that participate in the reaction pair, where $y_i(t)$ is the actual abundance, $\bar{y}_i$ is the equilibrium abundance determined from Eq. (25), and ε is a user-specified tolerance that will be taken to be the same for all species in the network.[6]

3.2.3 Reaction Vectors

A partial equilibrium approximation in a realistic large network could require that thousands or tens of thousands of reactions be examined for their equilibrium status at each timestep. It is useful to introduce a *reaction vector* formalism, adapted from the work of Mott [16, 18], that allows examination of partial equilibrium criteria in a particularly efficient way by exploiting the analogy of a reaction network to a linear vector space. This formalism will only be sketched here

[6] Alternatively, the equilibrium timescale (27) could be compared with the current numerical timestep to determine whether a reaction is near equilibrium: if τ is much smaller than the timestep, we may expect that equilibrium can be established and maintained in successive timesteps, even if it is being continually disturbed by other non-equilibrated processes.

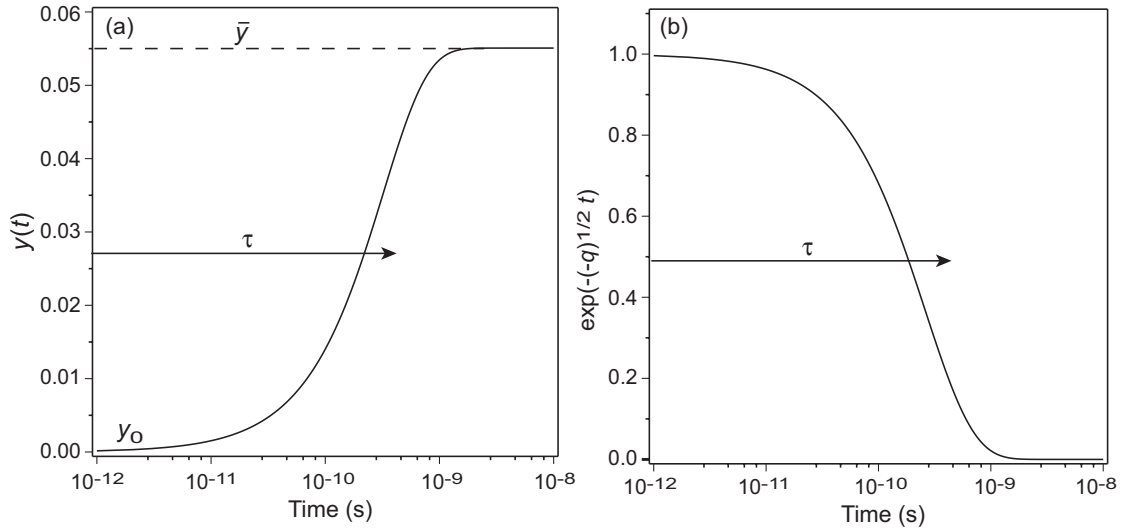

Figure 2: (a) Time evolution of the solution (24) assuming constant a, b, and c. The characteristic timescale for approach to equilibrium (27) is labeled τ and the equilibrium value of $y(t)$ defined by Eq. (25) is denoted by $\bar{y}$. To illustrate we have assumed the initial value $y_0 = 0$. For times considerably larger than τ the general solution (24) saturates at the equilibrium solution (25). If an integration timestep is much larger than τ, we may expect the reaction pair to become equilibrated over the timestep. (b) Behavior of the exponential factor in Eq. (24).

but is described fully in Ref. [10]. The concentration variables for the n species A_i in a network may be expressed as components of a composition vector

$$\boldsymbol{y} = (y_1, y_2, y_3, \ldots y_n), \tag{29}$$

which lies in an n-dimensional vector space Φ. The components y_i are proportional to number densities for the species labeled by A_i, so a specific vector in this space defines a particular composition. Any reaction in the network can then be written in the form

$$\sum_{i=1}^{n} a_i A_i \rightarrow \sum_{i=1}^{n} b_i A_i, \tag{30}$$

for some sets of coefficients $\{a_i\}$ and $\{b_i\}$. The coefficients on the two sides of the reaction (30) may then be used to define a *reaction vector* $\boldsymbol{r} \in \Phi$ with components

$$\boldsymbol{r} \equiv (b_1 - a_1, b_2 - a_2, \ldots, b_n - a_n), \tag{31}$$

that specifies how the composition may change because of the reaction. For a network with three or fewer species the corresponding linear vector space can be displayed geometrically. For example, Fig. 3 illustrates a network containing the isotopes $\{^4\mathrm{He}, ^8\mathrm{Be}, ^{12}\mathrm{C}\}$ and four reaction vectors corresponding to the reaction pairs $2\alpha \rightleftharpoons {}^8\mathrm{Be}$ and $\alpha + {}^8\mathrm{Be} \rightleftharpoons {}^{12}\mathrm{C}$. Larger networks cannot be visualized so easily, but their algebraic properties remain completely analogous to those of a simple network like that illustrated in Fig. 3.

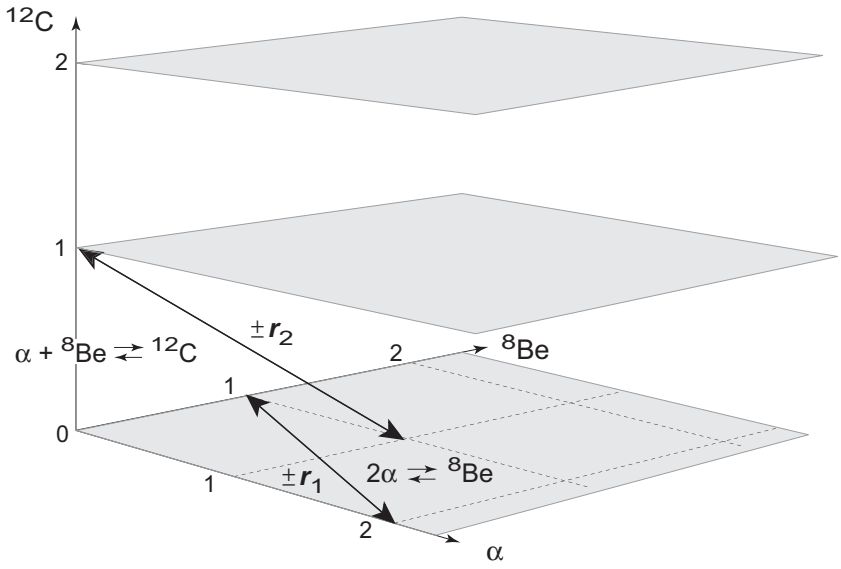

Figure 3: Four reaction vectors $\pm\boldsymbol{r}_1$ and $\pm\boldsymbol{r}_2$ for a 3-species network corresponding to the astrophysical triple-α process that converts ^{4}He to ^{12}C in red giant stars. Because there are three species in this network, three axes are required. The two reaction vectors $\pm\boldsymbol{r}_1$ describe the reaction pair $2\alpha \rightleftharpoons {}^8\mathrm{Be}$ because they convert a state with two α-particles to one with one ^{8}Be, or vice versa. Likewise, the two reaction vectors $\pm\boldsymbol{r}_2$ describe the reaction pair $\alpha + {}^8\mathrm{Be} \rightleftharpoons {}^{12}\mathrm{C}$.

3.2.4 Conservation Laws

It is easy to see that any vector in the network vector space that is *orthogonal to all reaction vectors* $\boldsymbol{r}_i$ is invariant under any possible reaction of the network. Therefore, such a vector is conserved and defines a *conservation law* for the system.[7] Some reaction networks, such as those for chemical kinetics, can have a number of conservation laws. For low-energy nuclear astrophysics the only conservation laws that follow from the structure of the network are usually associated with conservation of nucleon number.

3.2.5 Taxonomy of Generic Networks

Once a basis has been chosen for a specific reaction network it is straightforward then to enumerate

1. all possible *compositions* in terms of a set of vectors $\boldsymbol{y}_i$,
2. all possible *reactions* in terms of a set of vectors $\boldsymbol{r}_j$, and

[7] These conservation laws follow only from the structure of the network. The system may have additional conservation laws that follow from constraints not associated with the network structure.

Table 3: Reaction group classes

Class	Reaction pair	ReacLib class pairing
A	a $\rightleftharpoons$ b	1 with 1
B	a + b $\rightleftharpoons$ c	2 with 4
C	a +b + c $\rightleftharpoons$ d	3 with part of 8
D	a + b $\rightleftharpoons$ c + d	5 with 5
E	a + b $\rightleftharpoons$ c + d + e	6 with part of 8

3. all *conservation laws* that follow from the structure of the network in terms of a set of vectors $\boldsymbol{c}_k$.

This abstract description of a reaction network as a linear vector space retains a reference to a specific physical problem only through the choices of basis and allowed reaction vectors. Thus it facilitates development of generic methods to implement algebraically constrained explicit methods for diverse networks across multiple disciplines.

3.2.6 Reaction Groups

In the bookkeeping of the partial equilibrium approximation it will prove useful to leverage the reaction vector formalism discussed above and classify inverse reaction pairs into *reaction group classes* (*reaction groups,* or *RG* for short), in which all reactions of a group share the same reaction vector $\boldsymbol{r}$, up to a sign.[8] We shall employ the reaction classifications used in the ReacLib library [14] that are illustrated in Table 1. From this classification there are five independent ways to combine the reactions of Table 1 into reversible reaction pairs, leading to the reaction group classification illustrated in Table 3. For example, reaction group B consists of reactions from ReacLib reaction class 2 (a $\rightarrow$ b + c) paired with their inverse reactions (b + c $\rightarrow$ a), which belong to ReacLib reaction class 4.

For each reaction group class the characteristic differential equation governing the reaction pair considered in isolation is of the form given by Eq. (22), $dy/dt = ay^2 + by + c$, where y is either an abundance variable (proportional to a number density) for one of the reaction species, or a progress variable measuring the change from initial abundances associated with the reaction pair, and the coefficients a, b, and c are known parameters depending on the reaction rates that will be assumed constant within a single network timestep.[9]

[8] That is, the reactions in a reaction group are forward–backward paired so that each reaction in the group has a partner in the group that exactly undoes its action. The simplest example is a single forward–backward pair such as $a + b \rightleftharpoons c + d$, but there can be more than two members of a reaction group as long as they share the same reaction vector up to a sign. Two 2-member reaction groups, $\pm\boldsymbol{r}_1$ and $\pm\boldsymbol{r}_2$, were illustrated in Fig. 3.

[9] An exception occurs for reaction group classes C and E, where there are a 3-body reactions and the most general form of the differential equation governing the approach to equilibrium within a timestep involves cubic terms,

$$\frac{dy}{dt} = \alpha y^3 + \beta y^2 + \gamma y + \varepsilon.$$

These "3-body" reactions in astrophysics are typically sequential 2-body reactions and we assume that in any timestep $y(t)^3 \simeq y^{(0)} y(t)^2$, where $y^{(0)}$ is the (constant) value of $y(t)$ at the beginning of the timestep. This reduces the cubic

3.2.7 Equilibrium Constraints

If a reaction pair from a specific reaction group class is near equilibrium [as determined by Eq. (28)], there will be a corresponding equilibrium constraint that takes the general form [15]

$$\prod_{i=1}^{n} y_i^{(b_i - a_i)} = K, \tag{32}$$

where K is a ratio of rate parameters. For example, consider the reaction group class E pair $a + b \rightleftharpoons c + d + e$ in isolation, with differential equations for the populations y_i written in the form

$$\dot{y}_{\rm a} = \dot{y}_{\rm b} = -\dot{y}_{\rm c} = -\dot{y}_{\rm d} = -\dot{y}_{\rm e} = -k_{\rm f} y_a y_b + k_{\rm r} y_c y_d y_e.$$

Then at equilibrium, requiring that the forward flux $-k_{\rm f} y_a y_b$ and reverse flux $k_{\rm r} y_{\rm c} y_{\rm d} y_{\rm e}$ in the reaction pair sum to zero gives the constraint

$$\frac{y_a y_b}{y_c y_d y_e} = \frac{k_{\rm r}}{k_{\rm f}} \equiv K,$$

which is of the form (32).

3.2.8 Systematic Classification of Reaction Group Properties

Applying the principles discussed in the preceding paragraphs to the reaction group classes in Table 3 gives the results summarized for reaction group classes A–E in Appendix A. This reaction group classification has been developed assuming astrophysical thermonuclear networks and a particular parameterization (ReacLib) of the corresponding reaction rates. However, the illustrated methodology is of wider significance since for any large reaction network in any field the classification techniques illustrated here may be used to group all reactions of the network into reaction group classes and deduce for each reaction group class analytical expressions for all quantities necessary for applying a PE approximation. All that is required is to cast the network as a linear algebra problem by choosing a set of basis vectors corresponding to the species of the network, and then to define the corresponding reaction vectors and vectors implementing conservation laws of physical importance within this space. Once that is done, the formalism developed here may be applied systematically. In principle this classification bookkeeping need be developed only once for the networks of importance in any particular discipline, as illustrated here specifically for thermonuclear astrophysics networks.

3.3 General Methods for Algebraically Stabilized Explicit Calculations

We now have a set of tools to implement an explicit algebraic algorithm for solving stiff thermonuclear networks within the Endeve matrix framework. Let's sketch such an algorithm. Although our remarks will be specific to astrophysical thermonuclear networks, the basic approach should be relevant for a much broader range of problems.

equation to an effective quadratic equation of the form (22), with $a = \alpha y^{(0)} + \beta$, $b = \gamma$, and $c = \varepsilon$. Thus we describe the approach to equilibrium for all 1-body, 2-body, and 3-body reactions by an equation of the form (22).

3.3.1 Overview of Algorithm

We employ the partial equilibrium method (PE) in conjunction with either the asymptotic approximation (Asy) or the quasi-steady-state approximation (QSS). Once the reactions of the network are assigned to an abstract vector space and classified into reaction groups as described above, and we have chosen whether we will use the asymptotic or QSS approximations, advancing the integration by a single timestep has three components:

1. A numerical integration step begins with the full network of differential equations, but in computing fluxes all terms involving reaction groups judged to be equilibrated based on criteria defined by Eq. (28) evaluated for species populations at the end of the previous timestep are assumed to sum identically to zero net flux and are omitted from the summations generating the fluxes in Eq. (11).[10]

2. A trial timestep Δt is chosen according to criteria discussed in Section 3.4 below.

   (a) If the asymptotic approximation is being used the trial timestep is used in conjunction with the fluxes to determine which species in the network satisfy the stability condition $k\Delta t < \kappa$. For those that do the corresponding differential equation is updated by explicit forward Euler numerical integration. For those that don't ($k\Delta t \geq \kappa$), the corresponding population is updated algebraically using Eq. (14).

   (b) If instead the QSS approximation has been chosen, the trial timestep is used in conjunction with Eq. (19) to update populations for *all species in the network.*

   The accuracy criteria of the timestepping algorithm are then invoked to determine whether the error in the timestep is within tolerances. If so, the population updates are accepted. If not, the timestep is adjusted according to the timestepping criteria and the asymptotic or QSS repeated with the new timestep. If necessary this is iterated until the timestep is accepted.

3. For all species in reaction groups judged to be equilibrated at the beginning of the timestep, it is assumed that reactions not in equilibrium may have driven these populations slightly away from equilibrium during the timestep. If necessary these populations are adjusted slightly, subject to the system's conservation laws, to restore their equilibrium values at the end of the timestep.

Hence the partial equilibrium part of the approximation does not reduce the number of differential equations integrated numerically within a timestep, but instead removes systematically the stiffest parts of their fluxes (individual terms on the right sides of the differential equations). In contrast, the asymptotic approximation and the QSS approximation effectively reduce the number of differential equations integrated numerically by replacing the numerical forward difference with an analytically computed abundance for some (Asy) or all (QSS) isotopes. The

[10] The method is explicit, so calculations within each timestep depend only on the initial conditions set by results of the preceding timestep.

partial equilibrium and Asy/QSS approaches are complementary because partial equilibrium can operate microscopically to make the differential equation for a given isotope less stiff, even if that isotope does not satisfy Asy/QSS conditions, while the Asy/QSS approximations remove entire differential equations from the numerical update and thus can operate macroscopically to remove stiff reaction components, even if they do not satisfy partial equilibrium conditions. For brevity we may refer simply to the partial equilibrium (PE) approximation, but this always means the partial equilibrium approximation used in conjunction with either the asymptotic or the QSS approximation in the present context.

3.4 An Adaptive Timestepper for Explicit Algebraic Integration

Here we will use a suitably modified version of the timestepper developed for the neutrino transport code that implements the Endeve matrix formulation of the explicit algebraic method. A description is in preparation and will be added later.

4 Test Cases for Algebraically Stabilized Explicit Integration

This section outlines testing the use of explicit asymptotic (Asy), quasi-steady-state (QSS), and partial equilibrium (PE) methods for astrophysical thermonuclear networks. For astrophysical networks we shall replace the generic y_i of Eq. (1) with population variables common for astrophysics: the mass fraction X_i or the (molar) abundance Y_i, with

$$X_i = \frac{n_i A_i}{\rho N_{\rm A}} \qquad Y_i \equiv \frac{X_i}{A_i} = \frac{n_i}{\rho N_{\rm A}} \tag{33}$$

where $N_{\rm A}$ is Avogadro's number, ρ is the total mass density, A_i is the atomic mass number, n_i the number density for the species i, and conservation of nucleon number requires $\sum X_i = 1$.

4.1 Integration of the PP-Chains

The proton–proton chains (PP-chains) illustrated in Fig. 6 that convert hydrogen to helium and thereby power the Sun provide a spectacular illustration of stiffness in a simple yet physically-important network. Some rates important for the nuclear reactions in the PP chains computed from ReacLib are shown in Fig. 5. These are all 2-body reactions and the rates plotted correspond to $R^{\alpha}_{(2)}$ defined in Eq. (7b). The corresponding fluxes are then given by $M^{(2)}_{ij}$ defined in Eq. (11). A representative example of using the explicit algebraic approach in its original formulation is shown in Fig. 6, where the PP chains are integrated at a constant temperature and density characteristic of the current core of the Sun using the asymptotic method [7, 8] , the QSS method [7, 9], and the implicit backward-Euler code Xnet [19]. We see that the asymptotic and QSS integrations give results for the mass fractions in rather good agreement with the implicit code over 20 orders of magnitude, and generally take timesteps $dt \sim 0.1t$ that are comparable to those for the implicit code over the entire range of integration. The maximum stable timestep for a standard explicit integration method, which typically may be approximated by the inverse

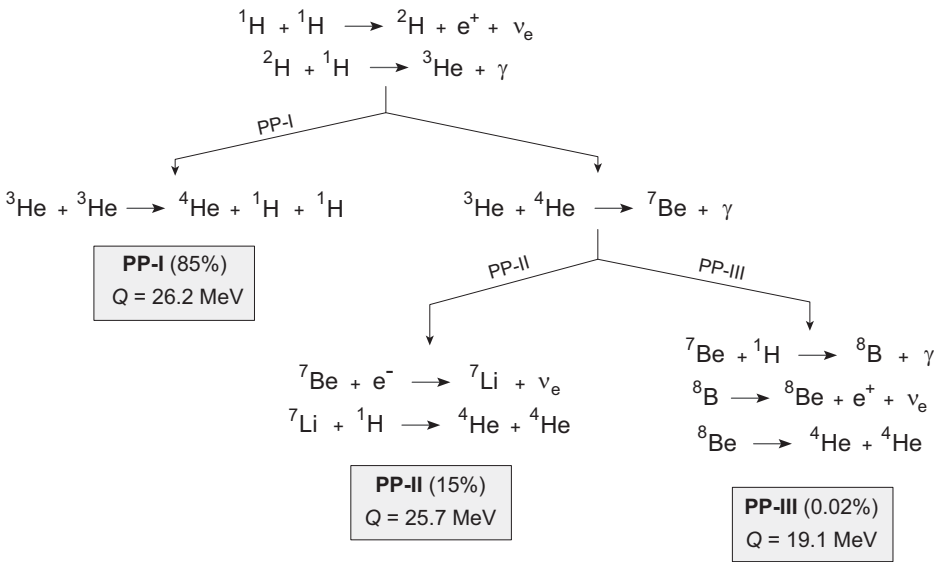

Figure 4: Main branches of the PP chains that power the Sun. The percentage contribution to current solar energy production and the effective Q-value (energy release) are shown for each branch of the chains.

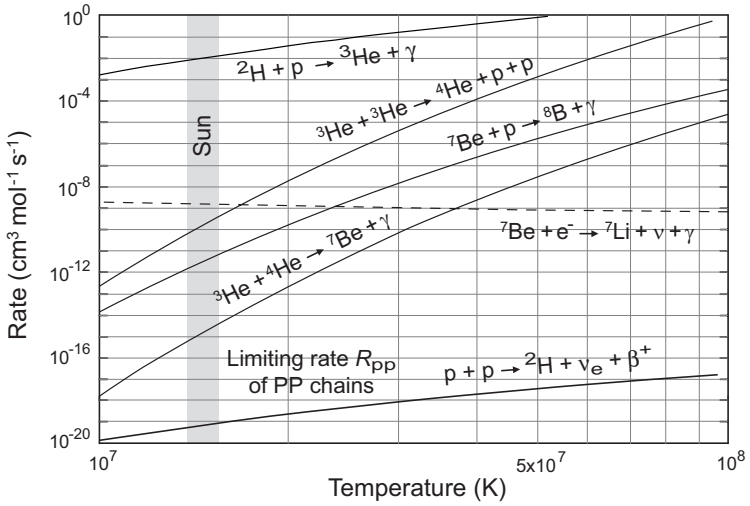

Figure 5: Reaction rates that are most important in PP-I, PP-II, and PP-III. Rates were obtained from the ReacLib compilation [14]. These are all 2-body reactions and the rates plotted correspond to $R^{\alpha}_{(2)}$ defined in Eq. (7b), with units $\mathrm{cm^3 mol^{-1} s^{-1}}$. The fluxes $M^{(2)}_{ij}$ given in Eq. (11) are then in units of $\mathrm{s^{-1}}$.

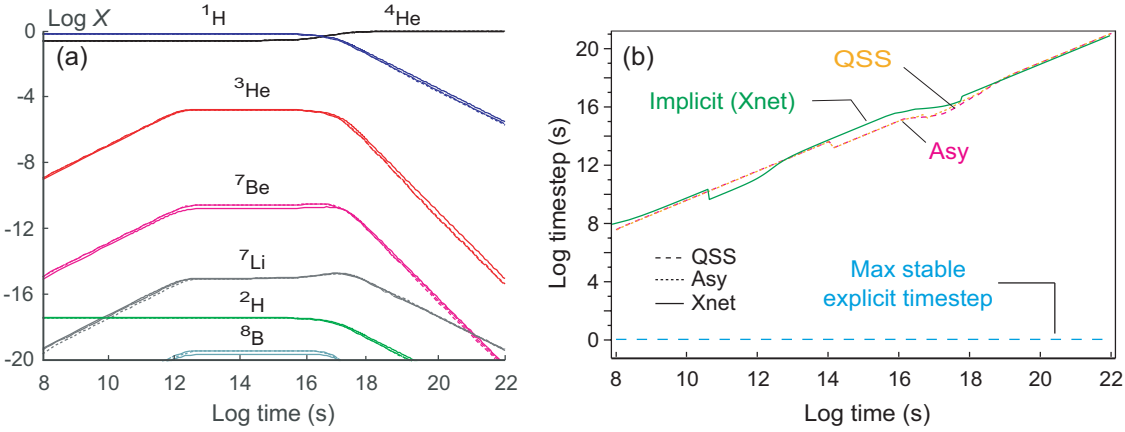

Figure 6: Integration of the PP chains at constant temperature $T_9 = 0.016$ (where T_9 denotes temperature in units of 10^9 K) and constant density 160 g cm^{-3}, assuming solar initial abundances. Reaction rates were taken from the ReacLib library [14]. (a) Mass fractions for the asymptotic method, the QSS method, and for the standard implicit code Xnet [19]. (b) Integration timesteps.

of the fastest rate in the system, is illustrated by the dashed blue curve in Fig. 6(b). Thus, at the end of the calculation the explicit integration timesteps are $\sim 10^{21}$ times larger than would be stable in a normal explicit integration. For a network this small the cost of matrix inversions in the implicit method adds little computational overhead and the implicit calculations require about the same overall computing time as the explicit Asy or QSS calculations.

4.2 Integration of Thermonuclear Alpha Networks

The PP chains example considered above does not encounter partial equilibrium conditions,[11] So asymptotic or QSS approximations are sufficient to integrate the PP chains efficiently. To test the asymptotic or QSS methods with partial equilibrium using the new matrix formulation we shall employ the alpha network (nuclear network containing only isotopes that differ from each other by multiples of the ^{4}He nucleus)

$$\{^4\mathrm{He}, ^{12}\mathrm{C}, ^{16}\mathrm{O}, ^{20}\mathrm{Ne}, ^{24}\mathrm{Mg}, ^{28}\mathrm{Si}, ^{32}\mathrm{S}, ^{36}\mathrm{Ar}, ^{40}\mathrm{Ca}, ^{44}\mathrm{Ti}, ^{48}\mathrm{Cr}, ^{52}\mathrm{Fe}, ^{56}\mathrm{Ni}, ^{60}\mathrm{Zn}, ^{64}\mathrm{Ge}, ^{68}\mathrm{Se}\} \quad (34)$$

that is displayed in Fig. 7, with the reactions and corresponding reaction groups given in Table 4. We shall concentrate on conditions expected in Type Ia supernova explosions.[12]

[11] This is because reactions inverse to those displayed in Fig. 6 have negligible rates for the conditions found in the present Sun.

[12] A Type Ia supernova is triggered by a thermonuclear runaway in electron-degenerate matter, for which temperatures can change at rates in excess of 10^{17} K s^{-1}. Such conditions lead to rapid equilibration of reaction groups in systems of extremely high stiffness and require the partial equilibrium approximation in conjunction with the asymptotic or QSS approximations to enable competitive explicit integration steps.

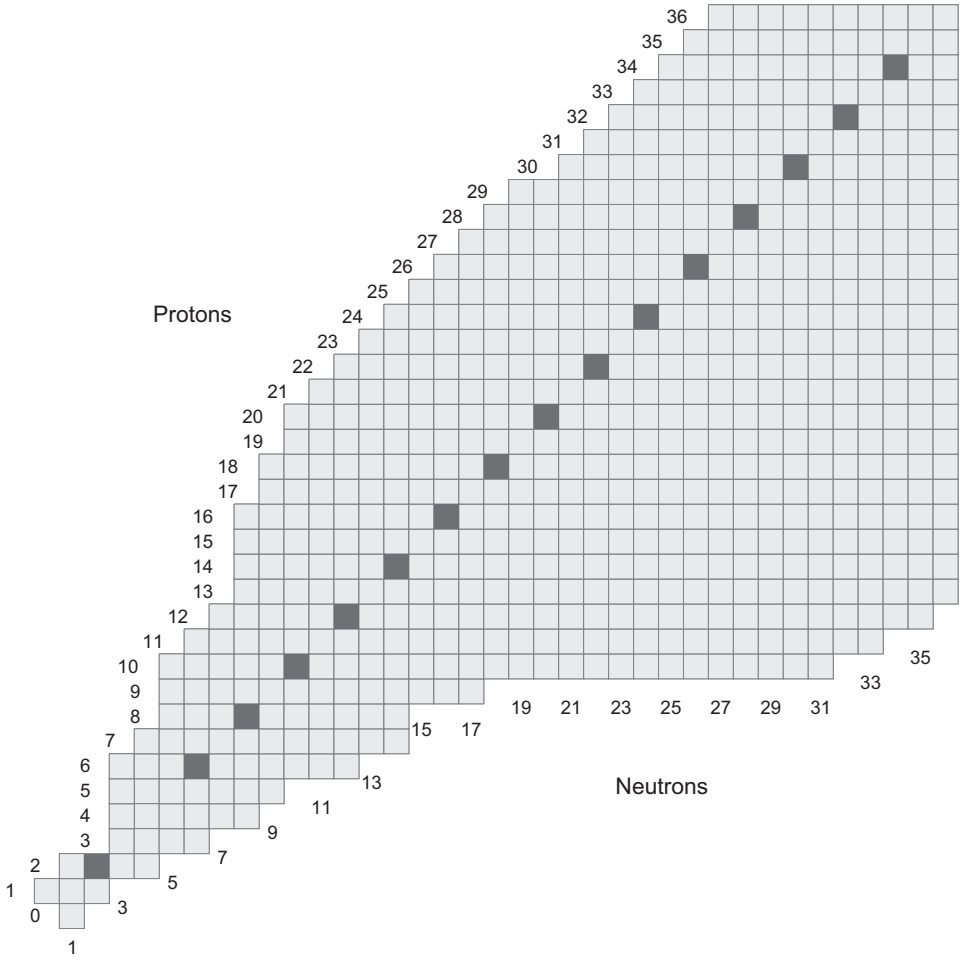

Figure 7: Isotopes of the α-network given in Eq. (34). Successive isotopes in the network are related by the capture or emission of ^{4}He (an α-particle). The isotope ^{8}Be (4 protons and 4 neutrons) is omitted because the ReacLib library views ^{8}Be as effectively two α-particles, by treating $3\alpha \leftrightharpoons \alpha + {}^8\text{Be} \leftrightharpoons {}^{12}\text{C}$ as the effective reaction group $3\alpha \leftrightharpoons {}^{12}\text{C}$ (the justification being that the mean life for ^{8}Be to decay into two α-particles in only $\sim 10^{-16}$ s).

4.2.1 Three-Species Alpha Network

Let's take as an initial test a toy alpha network including only three isotopes, ^{4}He (α-particles), ^{12}C, and ^{16}O, connected by the reactions $3\alpha \rightleftharpoons {}^{12}\text{C}$ and $\alpha + {}^{12}\text{C} \rightleftharpoons {}^{16}\text{O}$. By inspection the reactions may be classified into two reaction groups:

$$1:\ 3\alpha \rightleftharpoons {}^{12}\text{C} \qquad 2:\ \alpha + {}^{12}\text{C} \rightleftharpoons {}^{16}\text{O}. \tag{35}$$

Thus we have a total of four reactions in two reaction groups (RG), with RG 1 ($3\alpha \rightleftharpoons {}^{12}\text{C}$) belonging to reaction group class C and RG 2 ($\alpha + {}^{12}\text{C} \rightleftharpoons {}^{16}\text{O}$) belonging to reaction group

Table 4: Reactions of the alpha network for partial equilibrium calculations ($\alpha \equiv {}^4$He). The reverse reactions such as ${}^{20}\mathrm{Ne} \to \alpha + {}^{16}\mathrm{O}$ are photodisintegration reactions, $\gamma + {}^{20}\mathrm{Ne} \to \alpha + {}^{16}\mathrm{O}$, with the photon γ suppressed in the notation since we track only nuclear species in the network.

Group	Class	Reactions	Members
1	C	$3\alpha \rightleftharpoons {}^{12}\mathrm{C}$	4
2	B	$\alpha + {}^{12}\mathrm{C} \rightleftharpoons {}^{16}\mathrm{O}$	4
3	D	${}^{12}\mathrm{C} + {}^{12}\mathrm{C} \rightleftharpoons \alpha + {}^{20}\mathrm{Ne}$	2
4	B	$\alpha + {}^{16}\mathrm{O} \rightleftharpoons {}^{20}\mathrm{Ne}$	4
5	D	${}^{12}\mathrm{C} + {}^{16}\mathrm{O} \rightleftharpoons \alpha + {}^{24}\mathrm{Mg}$	2
6	D	${}^{16}\mathrm{O} + {}^{16}\mathrm{O} \rightleftharpoons \alpha + {}^{28}\mathrm{Si}$	2
7	B	$\alpha + {}^{20}\mathrm{Ne} \rightleftharpoons {}^{24}\mathrm{Mg}$	4
8	D	${}^{12}\mathrm{C} + {}^{20}\mathrm{Ne} \rightleftharpoons \alpha + {}^{28}\mathrm{Si}$	2
9	B	$\alpha + {}^{24}\mathrm{Mg} \rightleftharpoons {}^{28}\mathrm{Si}$	4
10	B	$\alpha + {}^{28}\mathrm{Si} \rightleftharpoons {}^{32}\mathrm{S}$	2
11	B	$\alpha + {}^{32}\mathrm{S} \rightleftharpoons {}^{36}\mathrm{Ar}$	2
12	B	$\alpha + {}^{36}\mathrm{Ar} \rightleftharpoons {}^{40}\mathrm{Ca}$	2
13	B	$\alpha + {}^{40}\mathrm{Ca} \rightleftharpoons {}^{44}\mathrm{Ti}$	2
14	B	$\alpha + {}^{44}\mathrm{Ti} \rightleftharpoons {}^{48}\mathrm{Cr}$	2
15	B	$\alpha + {}^{48}\mathrm{Cr} \rightleftharpoons {}^{52}\mathrm{Fe}$	2
16	B	$\alpha + {}^{52}\mathrm{Fe} \rightleftharpoons {}^{56}\mathrm{Ni}$	2
17	B	$\alpha + {}^{56}\mathrm{Ni} \rightleftharpoons {}^{60}\mathrm{Zn}$	2
18	B	$\alpha + {}^{60}\mathrm{Zn} \rightleftharpoons {}^{64}\mathrm{Ge}$	2
19	B	$\alpha + {}^{64}\mathrm{Ge} \rightleftharpoons {}^{68}\mathrm{Se}$	2

class B in Table 3. The partial equilibrium formulas for both cases have been summarized in Appendix A.

Differential Equations: The differential equations corresponding to this network may be written explicitly as

$$\dot{Y}_\alpha = -k_{\mathrm{f}}^{(1)} Y_\alpha^3 + k_{\mathrm{r}}^{(1)} Y_{12} - k_{\mathrm{f}}^{(2)} Y_\alpha Y_{12} + k_{\mathrm{r}}^{(2)} Y_{16} \tag{36a}$$

$$\dot{Y}_{12} = k_{\mathrm{f}}^{(1)} Y_\alpha^3 - k_{\mathrm{r}}^{(1)} Y_{12} - k_{\mathrm{f}}^{(2)} Y_\alpha Y_{12} + k_{\mathrm{r}}^{(2)} Y_{16} \tag{36b}$$

$$\dot{Y}_{16} = k_{\mathrm{r}}^{(1)} Y_\alpha Y_{12} - k_{\mathrm{r}}^{(1)} Y_{16} - k_{\mathrm{f}}^{(2)} Y_\alpha Y_{16} \tag{36c}$$

where $Y({}^{12}\mathrm{C}) \equiv Y_{12}$ and so on, and rate parameters $k_{\mathrm{f}}^{(n)}$ and $k_{\mathrm{r}}^{(n)}$ are shorthand for forward and reverse rates, respectively, for the reaction groups $n = 1, 2$ in Eq. (35). Although simple, this network exhibits most of the essential features of a realistic partial equilibrium calculation.

Matrix Formulation: Expressed in the matrix formalism of Eqs. (9)-(11), the network in Eqs. (36) become

$$\begin{pmatrix} \dot{Y}_\alpha \\ \dot{Y}_{12} \\ \dot{Y}_{16} \end{pmatrix} \equiv \begin{pmatrix} \dot{Y}_1 \\ \dot{Y}_2 \\ \dot{Y}_3 \end{pmatrix} = \begin{pmatrix} M_{11} & M_{12} & M_{13} \\ M_{21} & M_{22} & M_{23} \\ M_{31} & M_{32} & M_{33} \end{pmatrix} \begin{pmatrix} Y_1 \\ Y_2 \\ Y_3 \end{pmatrix}, \tag{37}$$

with the M_{ij} given by Eqs. (10) and (11). For example, from Eqs. (37) and (36),

$$\dot{Y}_\alpha = \dot{Y}_1 = M_{11}Y_1 + M_{12}Y_2 + M_{13}Y_3 = M_{11}Y_\alpha + M_{12}Y_{12} + M_{13}Y_{16},$$

where the M_{ij} are given by

$$M_{11} = -\tfrac{1}{2}\rho^2 R^{3\alpha\to{}^{12}\mathrm{C}} Y_\alpha^2 \qquad M_{12} = 3R^{{}^{12}\mathrm{C}\to 3\alpha} - \rho R^{\alpha+{}^{12}\mathrm{C}\to{}^{16}\mathrm{O}} Y_\alpha \qquad M_{13} = R^{{}^{16}\mathrm{O}\to\alpha+{}^{12}\mathrm{C}},$$

and where, for example, $R^{\alpha+{}^{12}\mathrm{C}\to{}^{16}\mathrm{O}}$ is the rate evaluated from Eq. (2) for the reaction $\alpha + {}^{12}\mathrm{C} \to {}^{16}\mathrm{O}$. Putting this together,

$$\dot{Y}_\alpha = -\big(\tfrac{1}{2}\rho^2 R^{3\alpha\to{}^{12}\mathrm{C}} Y_\alpha^2\big)Y_\alpha + \big(3R^{{}^{12}\mathrm{C}\to 3\alpha} - \rho R^{\alpha+{}^{12}\mathrm{C}\to{}^{16}\mathrm{O}} Y_\alpha\big)Y_{12} + R^{{}^{16}\mathrm{O}\to\alpha+{}^{12}\mathrm{C}} Y_{16},$$

which is Eq. (36a) if we define

$$k_\mathrm{f}^{(1)} \equiv \tfrac{1}{2}\rho^2 R^{3\alpha\to{}^{12}\mathrm{C}} \qquad k_\mathrm{r}^{(1)} \equiv 3R^{{}^{12}\mathrm{C}\to 3\alpha} \qquad k_\mathrm{f}^{(2)} \equiv \rho R^{\alpha+{}^{12}\mathrm{C}\to{}^{16}\mathrm{O}} \qquad k_\mathrm{r}^{(2)} \equiv R^{{}^{16}\mathrm{O}\to\alpha+{}^{12}\mathrm{C}}.$$

Likewise it may be verified that writing out the explicit equations for Y_{12} and Y_{16} implied by Eq. (37) leads to Eqs. (36b) and (36c).

Reaction Vectors and Reaction Group Classification: The reaction group classification in Eq. (35) may be obtained by inspection for this simple network, but it is useful to work it out formally in terms of vectors in the reaction vector space, since this provides a systematic way to classify reaction groups in more complex networks. Expressing the network in terms of a vector space as described in Section 3.2.3, the species composition vector $\boldsymbol{Y}$ may be defined as in Eq. (29),

$$\boldsymbol{Y} \equiv \begin{pmatrix} \alpha \\ {}^{12}\mathrm{C} \\ {}^{16}\mathrm{O} \end{pmatrix} \qquad Y_1 = Y_\alpha = \begin{pmatrix} 1 \\ 0 \\ 0 \end{pmatrix} \qquad Y_2 = Y_{12} = \begin{pmatrix} 0 \\ 1 \\ 0 \end{pmatrix} \qquad Y_3 = Y_{16} = \begin{pmatrix} 0 \\ 0 \\ 1 \end{pmatrix}. \tag{38}$$

Then, using Eqs. (30) and (31) the reactions of the network may be grouped into reaction vectors $\boldsymbol{r}$ as follows.

1. $3\alpha \leftrightharpoons {}^{12}\mathrm{C}$: Writing out Eq. (30) explicitly for this case,

$$\begin{aligned} \boldsymbol{r}_1 \equiv \boldsymbol{r}\big(3\alpha \to {}^{12}\mathrm{C}\big) &= (b_1 - a_1, b_2 - a_2, b_3 - a_3) \\ &= (0-3, 1-0, 0-0) \\ &= (-3, 1, 0) \\ \boldsymbol{r}_2 \equiv \boldsymbol{r}\big({}^{12}\mathrm{C} \to 3\alpha\big) &= (b_1 - a_1, b_2 - a_2, b_3 - a_3) \\ &= (3-0, 0-1, 0-0) \\ &= (3, -1, 0) \\ &= -\boldsymbol{r}_1 \end{aligned}$$

2. $\alpha + {}^{12}\mathrm{C} \leftrightharpoons {}^{16}\mathrm{O}$: As for above

$$\begin{aligned}
\boldsymbol{r}_3 \equiv \boldsymbol{r}\left(\alpha + {}^{12}\mathrm{C} \rightarrow {}^{16}\mathrm{O}\right) &= (b_1 - a_1, b_2 - a_2, b_3 - a_3) \\
&= (0-1, 0-1, 1-0) \\
&= (-1, -1, 1) \\
\boldsymbol{r}_4 \equiv \boldsymbol{r}\left({}^{16}\mathrm{O} \rightarrow \alpha + {}^{12}\mathrm{C}\right) &= (b_1 - a_1, b_2 - a_2, b_3 - a_3) \\
&= (1-0, 1-0, 0-1) \\
&= (1, 1, -1) \\
&= -\boldsymbol{r}_3
\end{aligned}$$

Therefore, since the formal definition of a reaction group is the set of all reactions within a network that, up to a sign, share the same reaction vector, $3\alpha \leftrightharpoons {}^{12}\mathrm{C}$ is one reaction group, with reaction vector $\pm(-3, 1, 0)$ and $\alpha + {}^{12}\mathrm{C} \leftrightharpoons {}^{16}\mathrm{O}$ is a second reaction group, with reaction vector $\pm(-1, -1, 1)$, which agrees with the classification in Eq. (35). This formal definition makes it easy to write computer code to assign reaction groups within an arbitrary network:

1. Assign an arbitrary vector basis for the species in the network as in Eqs. (29) or (38).
2. Use Eqs. (30) and (31) to compute reaction vectors $\boldsymbol{r}$ for each reaction permitted within the network.
3. Group reactions into reaction groups labeled by i that share the same reaction vectors $\pm\boldsymbol{r}_i$.

Now that all species and reactions in this network have been assigned vectors in the reaction network vector space, any possible reaction in the network is obtained by vector addition of the reaction vector with the initial species vector to give the final species vector. For example, writing the species vectors in Eq. (38) as row vectors for convenience and using the reaction vectors defined above,

$$ {}^{12}\mathrm{C} + (-\boldsymbol{r}_1) = (0,1,0) + (3,-1,0) = (3,0,0) = 3(1,0,0) = 3\alpha $$

is the vector addition equation corresponding to the reaction ${}^{12}\mathrm{C} \rightarrow 3\alpha$ and

$$ (\alpha + {}^{12}\mathrm{C}) + \boldsymbol{r}_3 = (1,0,0) + (0,1,0) + (-1,-1,1) = (0,0,1) = {}^{16}\mathrm{O} $$

is the vector addition equation corresponding to the reaction $\alpha + {}^{12}\mathrm{C} \rightarrow {}^{16}\mathrm{O}$. Figure Fig. 8 illustrates the reaction vector space for this 3-isotope network.

Example Result from Original Explicit Algebraic Formulation: Figures 9 and 12 illustrate a simulation with this network at a constant temperature of 5×10^9 K and constant density 1×10^8 g cm^{-3} using the original formulation of the explicit algebraic approach [10]. This calculation employs the explicit asymptotic method, but imposes partial equilibrium constraints if the abundances of all reactions in a reaction group are within 0.01 of their equilibrium abundances. A deeper understanding of the factors that determine the timesteps in Fig. 9 may be obtained by

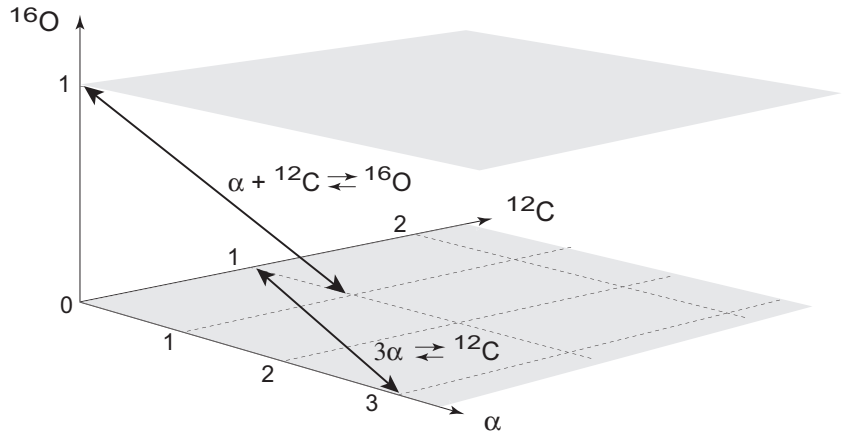

Figure 8: The reaction vector space for the network containing α-particles, ^{12}C, and ^{16}O, connected by the reactions $3\alpha \rightleftharpoons {}^{12}\mathrm{C}$ and $\alpha + {}^{12}\mathrm{C} \rightleftharpoons {}^{16}\mathrm{O}$. The two reaction groups are indicated by the double-ended arrows.

consulting Fig. 13, which displays all timescales relevant for the problem as a function of time. Figure 13(a) shows the timescales defined by the inverse of the reaction rates for all reactions in the network (dotted and dashed curves), the timescales τ of Eq. (27) for establishing equilibrium for the two reaction groups in this calculation (magenta and blue bands), and the integration timestepping for various methods (solid curves).

4.2.2 Full Alpha Network

For a more realistic test case let's assume an alpha network with a constant temperature of $T_9 = 7$ (that is, $T = 10^9$ K), a constant density of 10^8 g cm^{-3}, the 16-isotope network displayed in Eq. (34) and Fig. 7, and the reaction group classifications displayed in Table 4. A calculation for this case made in the original formulation of the explicit algebraic formalism is shown in Fig. 16. In this calculation ReacLib [14] was used for all rates except that inverse rates for reaction groups 3, 5, and 6 are not included in the standard ReacLib tabulation and were taken from Ref. [20]. For all calculations the equilibrium criteria were imposed using Eq. (28), with a constant value $\varepsilon_i = 0.01$ for the tolerance parameter. As shown in Fig. 17(a) the timesteps required for the asymptotic + partial equilibrium and implicit calculations were about the same but because the explicit algebraic code can do each timestep faster the Asy+PE calculation was estimated to be ~ 3 times faster than the implicit code, even for this small 16-isotope network. In contrast, the asymptotic method used alone lags far behind the implicit calculation at late times because partial equilibration becomes significant after $\sim 10^{-8}$ s, as illustrated in Fig. 17(b).

4.3 Scaling with Network Size

For an explicit method no matrix inversions are required and the time to compute should scale linearly with the size of the network if the matrix is relatively sparse (generally true for large

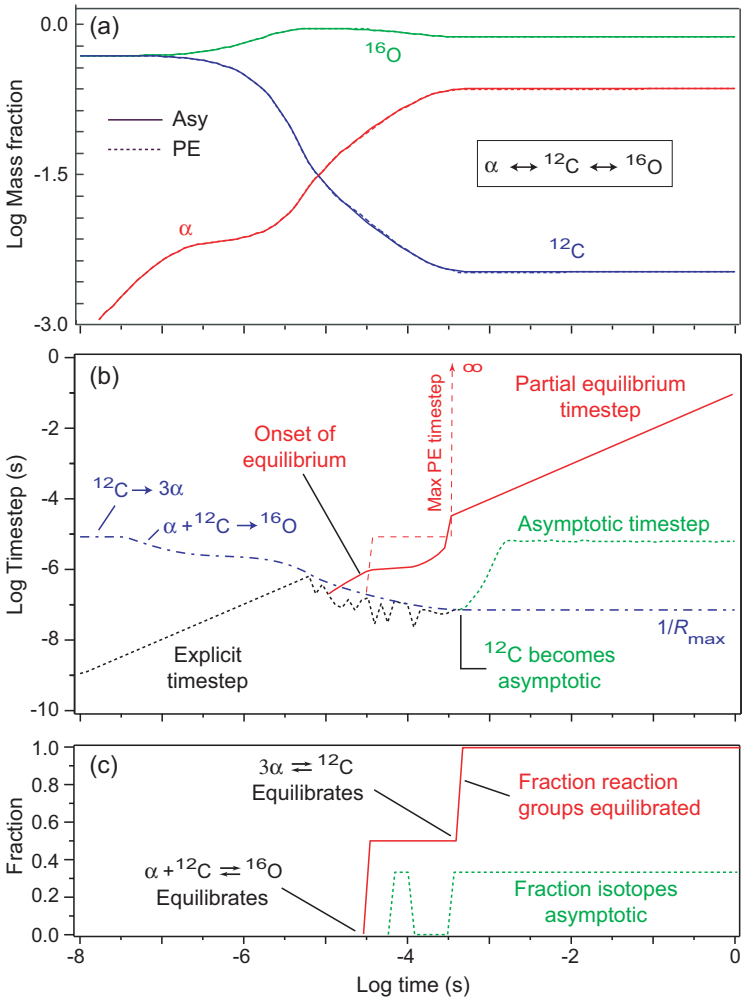

Figure 9: The effect of imposing partial equilibrium on integration timesteps for the network $\alpha \rightleftharpoons {}^{12}\mathrm{C} \rightleftharpoons {}^{16}\mathrm{O}$ at a constant temperature of 5×10^9 K and constant density 1×10^8 g cm^{-3}, assuming initial mass fractions of 0.50 for ^{12}C and ^{16}O. Reaction rates were taken from ReacLib [14]. (a) Evolution of mass fractions. The results are almost indistinguishable between the purely asymptotic calculation (Asy) and the asymptotic plus partial equilibrium calculation (PE). (b) The purely-explicit integration timestep (black dotted), the asymptotic timestep (green dotted), the partial equilibrium timestep (solid red), the approximate maximum explicit timestep for the asymptotic calculation (dash-dotted blue), and the maximum stable timestep for the partial equilibrium calculation (dashed red). (c) The fraction of isotopes that are asymptotic and the fraction of reaction groups that are equilibrated as a function of time. The dotted green curves in the middle and bottom figures refer to the results obtained with the explicit asymptotic method if partial equilibrium is not imposed. The curve labeled $1/R_{\mathrm{max}}$ indicates the maximum stable timestep for a standard explicit method like forward Euler. At the end of the calculation the Asy + PE calculation is taking stable and accurate timesteps that are 10^4 times larger than for a purely asymptotic calculation and 10^6 times larger than for a forward Euler calculation.

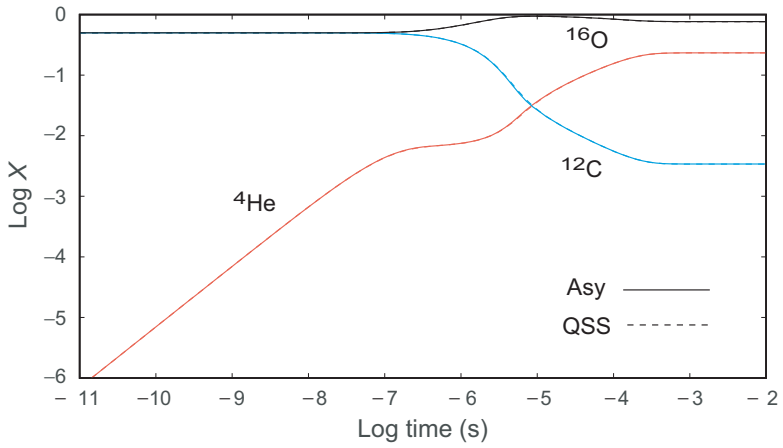

Figure 10: Mass fraction for the calculation in Fig. 9 for Asy and QSS methods.

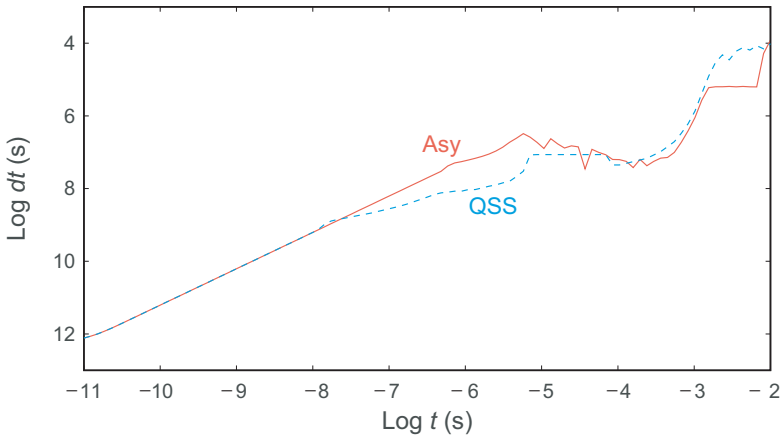

Figure 11: Timesteps for the calculation in Fig. 9 for Asy and QSS methods.

thermonuclear networks). Figure 18 demonstrates linear scaling for two cases using the original formulation of the explicit algebraic approach. The QSS algorithm is similar to the Asy algorithm and should also scale linearly. The partial equilibrium method adds some additional computation and logic to the asymptotic or QSS methods but adds no matrix inversions so the PE method should not alter appreciably the linear scaling of Asy or QSS. Since the new matrix implementation of the explicit algebraic method is in essence a more efficient and transparent re-packaging of the original algorithm, it may be expected to scale linearly also for sparse thermonuclear networks.

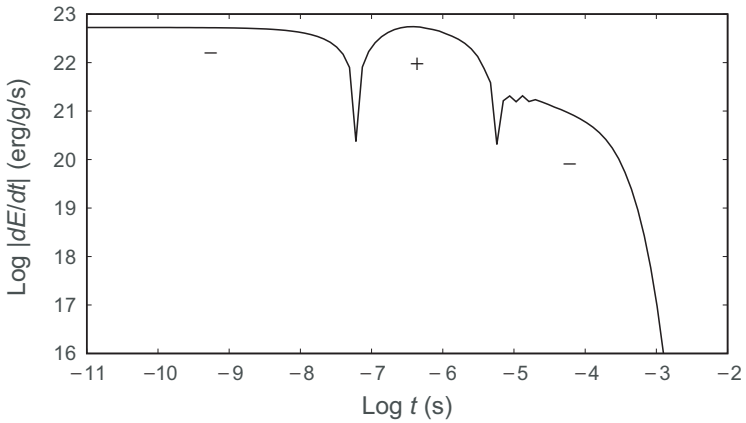

Figure 12: Differential energy release for the calculation in Fig. 9. The rate of energy production dE/dt can be positive or negative so the log of the absolute value is plotted, with signs indicated.

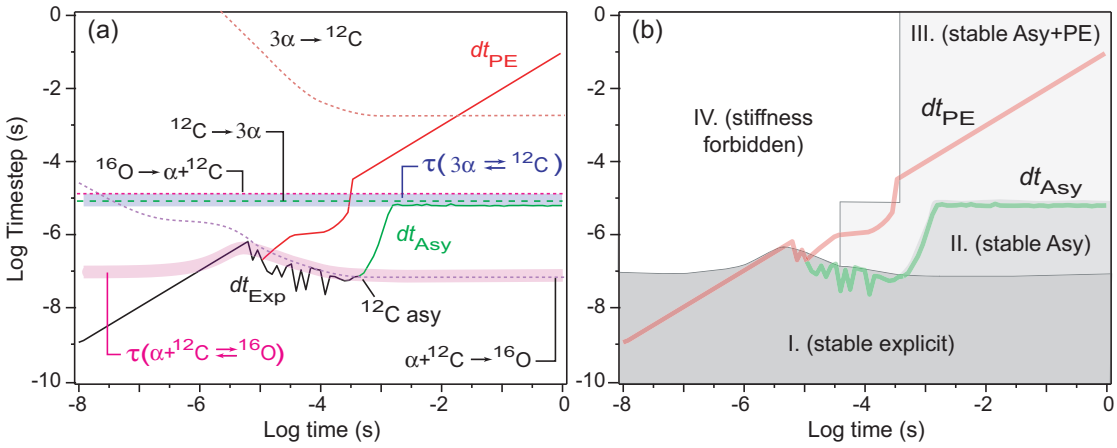

Figure 13: (a) Equilibration and reaction timescales for Fig. 9. (b) Stiffness stability domains implied by the equilibration timescales in part (a). All timesteps in region I are stable for forward Euler explicit integration. All timesteps in region II are stable for the asymptotoic (Asy) approximation. All timesteps in region III are stable for the asymptotic approximation supplemented by the partial equilibrium approximation (Asy+PE). Timesteps in region IV are potentially unstable for all of these explicit algebraic methods, but timesteps as large as those in region IV are probably not of interest for accuracy reasons, even if they were stable.

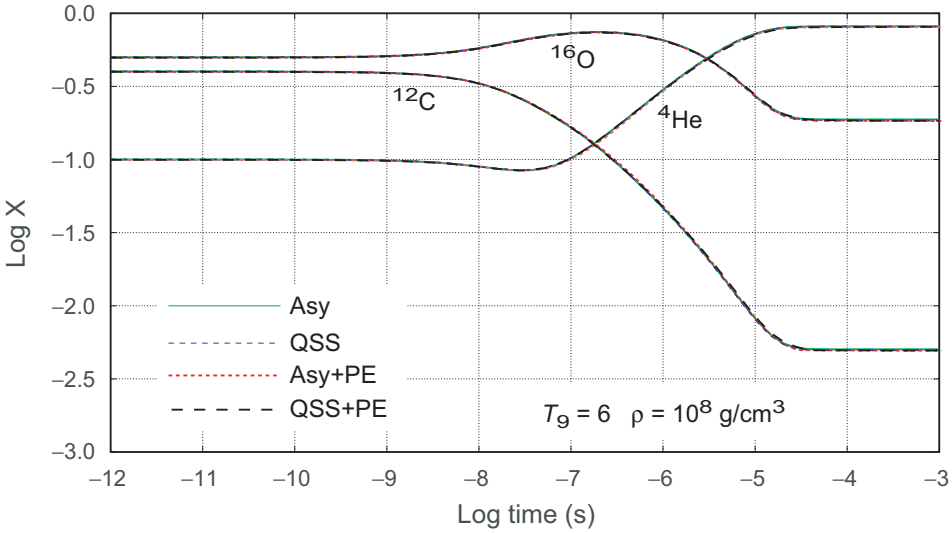

Figure 14: Mass fractions for the network $\alpha \rightleftharpoons {}^{12}\mathrm{C} \rightleftharpoons {}^{16}\mathrm{O}$ at a constant temperature of 6×10^9 K and constant density 1×10^8 g cm^{-3}, assuming initial mass fractions of 0.1 for ^{4}He, 0.40 for ^{12}C, and 0.5 for ^{16}O. Reaction rates were taken from ReacLib [14].

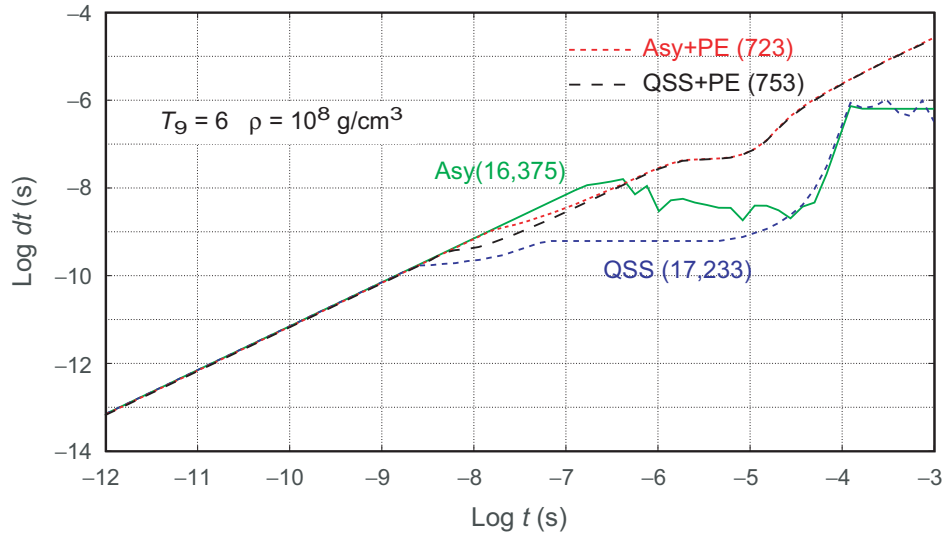

Figure 15: Integration timesteps for the reaction displayed in Fig. 14 for the asymptotic (Asy), quasi-steady-state (QSS) and asymptotic plus partial equilibrium (Asy+PE) algebraic explicit methods. The total number of integration steps for the four methods are shown in parentheses. Adding the partial equilibrium approximation to the Asy and QSS methods reduces the number of integration steps by a factor of almost 23.

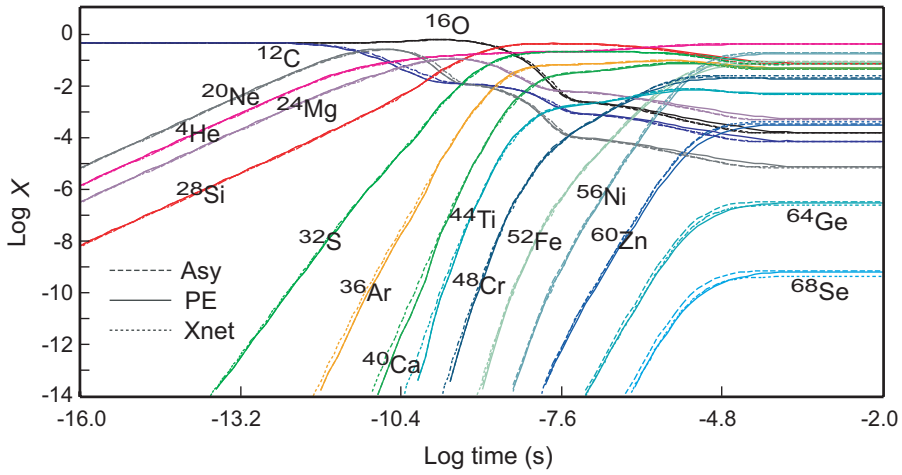

Figure 16: Alpha network mass fractions for partial equilibrium calculation with constant $T_9 = 7$ and $\rho = 1 \times 10^8$ g cm^{-3}. Solid curves are asymptotic + PE, dashed curves are asymptotic, and dotted curves are implicit (Xnet).

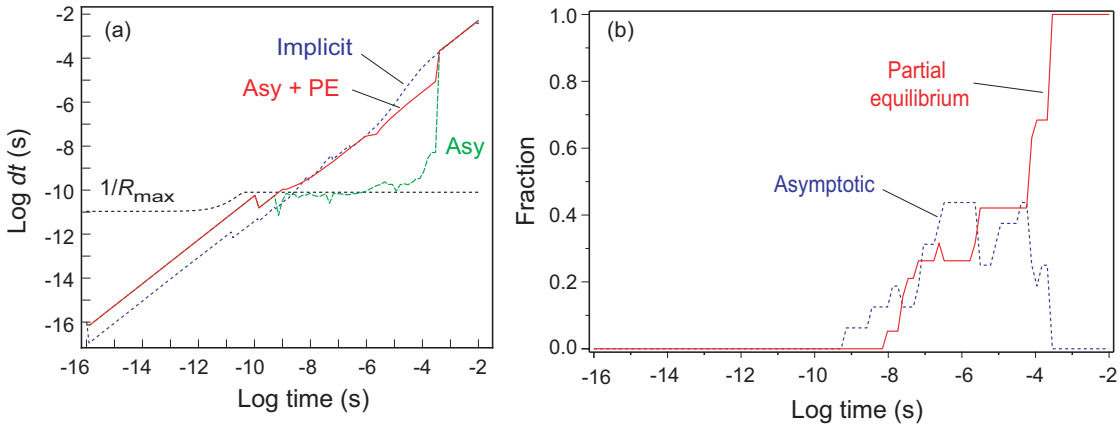

Figure 17: (a) Integration timesteps for asymptotic plus partial equilibrium calculation (solid red), the implicit code Xnet [19] (dotted blue), and the asymptotic method of Ref. [8] (dashed green) for the case in Fig. 16. The curve labeled $1/R_{\max}$ is the maximum stable timestep for a standard (not algebraically stabilized) explicit method. (b) Onset of asymptotic and partial equilibrium conditions as a function of time for the calculation in Fig. 16. The dotted curve is the fraction of isotopes satisfying the asymptotic condition. The solid curve is the fraction of reaction groups satisfying the partial equilibrium condition. Note that the system reaches complete equilibrium through a series of partial equilibrations beginning about 10^8 s after initiation of the explosion.

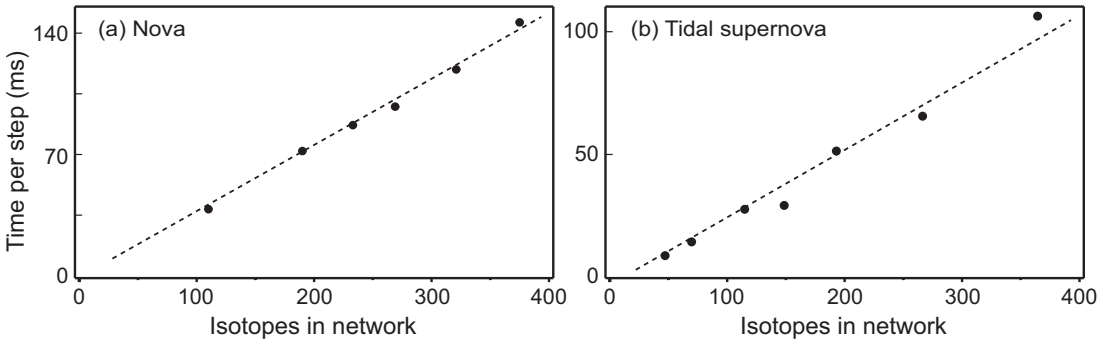

Figure 18: Linear scaling of wall clock time per integration step with number of isotopes in the network for the explicit asymptotic approximation [7]. (a) A nova simulation. (b) A tidal supernova simulation.

A Reaction Group Classification

Applying the principles discussed in Section 3.2 to the reaction group classes in Table 3 gives the following partial equilibrium properties of reaction group classes for astrophysical thermonuclear networks.

Reaction Group Class A (a $\rightleftharpoons$ b)

Source term: $\frac{dy_a}{dt} = -k_{\rm f} y_a + k_{\rm r} y_b$ Constraints: $y_a + y_b \equiv c_1 = y_a^0 + y_b^0$

Equation: $\frac{dy_a}{dt} = b y_a + c \quad b = -k_{\rm f} \quad c = k_{\rm r}$ Solution: $y_a(t) = y_a^0 e^{bt} - \frac{c}{b}\left(1 - e^{bt}\right)$

Equil. solution: $\bar{y}_a = -\frac{c}{b} = \frac{k_{\rm r}}{k_{\rm f}}$ Equil. timescale: $\tau = \frac{1}{b} = \frac{1}{k_{\rm f}}$

Equil. tests: $\frac{|y_i - \bar{y}_i|}{\bar{y}_i} < \varepsilon_i \;\; (i = a, b)$ Equil. constraint: $\frac{y_a}{y_b} = \frac{k_{\rm r}}{k_{\rm f}}$

Other variables: $y_b = c_1 - y_a$

Progress variable: $\lambda \equiv y_a^0 - y_a \quad y_a = y_a^0 - \lambda \quad y_b = y_b^0 + \lambda$

Reaction Group Class B (a + b $\rightleftharpoons$ c)

Source term: $\frac{dy_a}{dt} = -k_{\rm f} y_a y_b + k_{\rm r} y_c$

Constraints: $y_b - y_a \equiv c_1 = y_b^0 - y_a^0 \quad y_b + y_c \equiv c_2 = y_b^0 + y_c^0$

Equation: $\frac{dy_a}{dt} = a y_a^2 + b y_a + c \quad a = -k_{\rm f} \quad b = -(c_1 k_{\rm f} + k_b) \quad c = k_{\rm r}(c_2 - c_1)$

Solution: Eq. (24) Equil. solution: Eq. (25) Equil. timescale: Eq. (27)

Equil. tests: $\frac{|y_i - \bar{y}_i|}{\bar{y}_i} < \varepsilon_i \;\; (i = a, b, c)$ Equil. constraint: $\frac{y_a y_b}{y_c} = \frac{k_{\rm r}}{k_{\rm f}}$

Other variables: $y_b = c_1 + y_a \quad y_c = c_2 - y_b$

Progress variable: $\lambda \equiv y_a^0 - y_a \quad y_a = y_a^0 - \lambda \quad y_b = y_b^0 - \lambda \quad y_c = y_c^0 + \lambda$

Reaction Group Class C (a + b + c $\rightleftharpoons$ d)

Source term: $\frac{dy_a}{dt} = -k_{\rm f} y_a y_b y_c + k_{\rm r} y_d$ Constraints: $y_a - y_b \equiv c_1 = y_a^0 - y_b^0$

$\frac{1}{3}(y_a + y_b + y_c) + y_d \equiv c_3 = \frac{1}{3}(y_a^0 + y_b^0 + y_c^0) + y_d^0 \quad y_a - y_c \equiv c_2 = y_a^0 - y_c^0$

Equation: $\frac{dy_a}{dt} = a y_a^2 + b y_a + c$

$a = -k_{\rm f} y_a^0 + k_{\rm f}(c_1 + c_2) \quad b = -(k_{\rm f} c_1 c_2 + k_{\rm r}) \quad c = (c_3 + \frac{1}{3}c_1 + \frac{1}{3}c_2) k_{\rm r}$

Solution: Eq. (24) Equil. solution: Eq. (25) Equil. timescale: Eq. (27)

Equil. tests: $\frac{|y_i - \bar{y}_i|}{\bar{y}_i} < \varepsilon_i \;\; (i = a, b, c, d)$ Equil. constraint: $\frac{y_a y_b y_c}{y_d} = \frac{k_{\rm r}}{k_{\rm f}}$

Other variables: $y_b = y_a - c_1 \quad y_c = y_a - c_2 \quad y_d = c_3 - y_a + \frac{1}{3}(c_1 + c_2)$

Progress variable: $\lambda \equiv y_a^0 - y_a \quad y_a = y_a^0 - \lambda \quad y_b = y_b^0 - \lambda \quad y_c = y_c^0 - \lambda$

$y_d = \lambda + y_d^0$

Reaction Group Class D (a + b $\rightleftharpoons$ c + d)

Source term: $\frac{dy_a}{dt} = -k_\mathrm{f} y_a y_b + k_\mathrm{r} y_c y_d$ Constraints: $y_a - y_b \equiv c_1 = y_a^0 - y_b^0$

$y_a + y_c \equiv c_2 = y_a^0 + y_c^0 \quad y_a + y_d \equiv c_3 = y_a^0 + y_d^0$

Equation: $\frac{dy_a}{dt} = a y_a^2 + b y_a + c \quad a = k_\mathrm{r} - k_\mathrm{f} \quad b = -k_\mathrm{r}(c_2 + c_3) + k_\mathrm{f} c_1 \quad c = k_\mathrm{r} c_2 c_3$

Solution: Eq. (24) Equil. solution: Eq. (25) Equil. timescale: Eq. (27)

Equil. tests: $\frac{|y_i - \bar{y}_i|}{\bar{y}_i} < \varepsilon_i \;\; (i = a,b,c,d)$ Equil. constraint: $\frac{y_a y_b}{y_c y_d} = \frac{k_\mathrm{r}}{k_\mathrm{f}}$

Other variables: $y_b = y_a - c_1 \quad y_c = c_2 - y_a \quad y_d = c_3 - y_a$

Progress variable: $\lambda \equiv y_a^0 - y_a \quad y_a = y_a^0 - \lambda \quad y_b = y_b^0 - \lambda \quad y_c = y_c^0 + \lambda \quad y_d = y_d^0 + \lambda$

Reaction Group Class E (a + b $\rightleftharpoons$ c + d + e)

Source term: $\frac{dy_a}{dt} = -k_\mathrm{f} y_a y_b + k_\mathrm{r} y_c y_d y_e$

Constraints: $y_a + \frac{1}{3}(y_c + y_d + y_e) \equiv c_1 = y_a^0 + \frac{1}{3}(y_c^0 + y_d^0 + y_e^0)$

$y_a - y_b \equiv c_2 = y_a^0 - y_b^0 \quad y_c - y_d \equiv c_3 = y_c^0 - y_d^0 \quad y_c - y_e \equiv c_4 = y_c^0 - y_e^0$

Equation: $\frac{dy_a}{dt} = a y_a^2 + b y_a + c$

$a = (3c_1 - y_a^0) k_\mathrm{r} - k_\mathrm{f} \quad b = c_2 k_\mathrm{f} - (\alpha\beta + \alpha\gamma + \beta\gamma) k_\mathrm{r} \quad c = k_\mathrm{r} \alpha\beta\gamma$

$\alpha \equiv c_1 + \frac{1}{3}(c_3 + c_4) \quad \beta \equiv c_1 - \frac{2}{3}c_3 + \frac{1}{3}c_4 \quad \gamma \equiv c_1 + \frac{1}{3}c_3 - \frac{2}{3}c_4$

Solution: Eq. (24) Equil. solution: Eq. (25) Equil. timescale: Eq. (27)

Equil. tests: $\frac{|y_i - \bar{y}_i|}{\bar{y}_i} < \varepsilon_i \;\; (i = a,b,c,d,e)$ Equil. constraint: $\frac{y_a y_b}{y_c y_d y_e} = \frac{k_\mathrm{r}}{k_\mathrm{f}}$

Other variables: $y_b = y_a - c_2 \quad y_c = \alpha - y_a \quad y_d = \beta - y_a \quad y_e = \gamma - y_a$

Progress variable: $\lambda \equiv y_a^0 - y_a \quad y_a = y_a^0 - \lambda \quad y_b = y_b^0 - \lambda \quad y_c = y_c^0 + \lambda$

$y_d = y_d^0 + \lambda \quad y_e = y_e^0 + \lambda$

We have allowed the possibility of a different ε_i for each species i but in practice one would often choose the same small value ε for all i. A typical choice is $\varepsilon_i = 0.01$ for all species.

References

[1] E.S. Oran and J.P. Boris, Numerical Simulation of Reactive Flow, Cambridge University Press, 2005.

[2] C.W. Gear, Numerical Initial Value Problems in Ordinary Differential Equations, Prentice Hall, 1971.

[3] J.D. Lambert, Numerical Methods for Ordinary Differential Equations, Wiley, 1991.

[4] W.H. Press, S.A. Teukolsky, W.T. Vettering, and B.P. Flannery, Numerical Recipes in Fortran, Cambridge University Press, 1992.

[5] W.R. Hix and B.S. Meyer, Thermonuclear kinetics in astrophysics, Nuc. Phys. A 777 (2006) 188-207.

[6] F.X. Timmes, Integration of Nuclear Reaction Networks for Stellar Hydrodynamics, ApJS 124 (1999) 241-263.

[7] Mike Guidry, J. Comp. Phys. **231**, 5266-5288 (2012). [arXiv:1112.4778].

[8] M. W. Guidry, R. Budiardja, E. Feger, J. J. Billings, W. R. Hix, O. E. B. Messer, K. J. Roche, E. McMahon, and M. He, Comput. Sci. Disc. **6**, 015001 (2013) [arXiv: 1112.4716].

[9] M. W. Guidry and J. A. Harris, Comput. Sci. Disc. **6**, 015002 (2013) [arXiv: 1112.4750]

[10] M. W. Guidry, J. J. Billings, and W. R. Hix, Comput. Sci. Disc. **6**, 015003 (2013) [arXiv: 1112.4738]

[11] Benjamin Brock, Andrew Belt, Jay Jay Billings, and Mike Guidry, J. Comp. Phys. **302**, 591-602 (2015).

[12] A. Haidar, B. Brock, S. Tomov, M. Guidry, J. J. Billings, D. Shyles, and J. Dongarra, "Performance Analysis and Acceleration of Explicit Integration for Large Kinetic Networks using Batched GPU Computations" 2016 IEEE High Performance Extreme Computing Conference, HPEC (2016).

[13] E. Endeve et al, unpublished.

[14] T. Rauscher and F.-K. Thielemann, Astrophysical Reaction Rates From Statistical Model Calculations, At. Data Nuclear Data Tables 75 (2000) 1-351.

[15] D.R. Mott, E.S. Oran, and B. van Leer, Differential Equations of Reaction Kinetics, J. Comp. Phys. 164 (2000) 407-428.

[16] D.R. Mott, New Quasi-Steady-State and Partial-Equilibrium Methods for Integrating Chemically Reacting Systems, doctoral thesis, University of Michigan, 1999.

[17] E. Feger, Evaluating Explicit Methods for Solving Astrophysical Nuclear Reaction Networks, doctoral thesis, University of Tennessee, 2011.

[18] D. Mott, E. Oran, and B. van Leer, Identifying and Imposing Partial Equilibrium in Chemically Reacting Systems, in AIAA-2003-667, 41st Aerospace Sciences Meeting and Exhibit, Reno, Nevada, 2003.

[19] W.R. Hix and F.-K. Thielemann, Computational methods for nucleosynthesis and nuclear energy generation, J. Comp. Appl. Math. 109 (1999) 321-351.

[20] Tabulated at http://groups.nscl.msu.edu/jina/reaclib/db/. The JINA extensions to ReacLib are discussed in R.H. Cyburt, et al., The JINA ReacLib Database:Its Recent Updates and Impact on Type-I X-ray Bursts, Ap. J. Supp. 189 (2010) 240-252.